Journal of Encapsulation and Adsorption Sciences, 2024, 12, 1-24
https://www.scirp.org/journal/jeas
ISSN Online: 2161-4873
ISSN Print: 2161-4865

Simultaneous Adsorption of Aqueous Pb^{2+}, Cu^{2+}, Zn^{2+}, and Cd^{2+} Using Surfactant-Modified and Unmodified Activated Carbon in a Fixed Bed Column

Morufu A. Olatunji[1,2], Kamoru A. Salam[1*], Abdullahi M. Evuti[1]

[1]Department of Chemical Engineering, University of Abuja, Abuja, Nigeria
[2]National Agency for Science and Engineering Infrastructure (NASENI), Abuja, Nigeria
Email: *kamoru.salam@uniabuja.edu.ng

How to cite this paper: Olatunji, M.A., Salam, K.A. and Evuti, A.M. (2024) Simultaneous Adsorption of Aqueous Pb^{2+}, Cu^{2+}, Zn^{2+}, and Cd^{2+} Using Surfactant-Modified and Unmodified Activated Carbon in a Fixed Bed Column. *Journal of Encapsulation and Adsorption Sciences*, **12**, 1-24.
https://doi.org/10.4236/jeas.2024.121001

Received: August 19, 2024
Accepted: September 17, 2024
Published: September 20, 2024

Abstract

The goal of this work is to improve the simultaneous removal of Pb^{2+}, Cu^{2+}, Zn^{2+}, and Cd^{2+} ions from synthetic wastewater in a fixed bed column by incorporating sodium dodecyl sulfate (SDS) onto the surface of activated carbon made from coconut shells. The activated carbons were characterized using Fourier transform infrared spectroscopy (FT-IR) and scanning electron microscopy-energy dispersive x-ray (SEM-EDX). The adsorption column dynamics were studied by varying the flow rates (5, 10 and 15 mL/min), bed heights (10, 15 and 20 cm), and initial concentrations (50, 150, and 250 mg/L). The activated carbon has a pore volume of 0.715 cm^3/g and a BET-specific surface area of 1410 m^2/g. Sodium dodecyl sulfate (SDS) surfactant incorporation onto the surface of the activated carbon enhances its capacity for simultaneous adsorption of Pb^{2+}, Cu^{2+}, Zn^{2+}, and Cd^{2+} from the aqueous medium. The affinity of the heavy metals to both unmodified (AC) and modified (AC-SDS) activated carbons followed the order of $Pb^{2+} > Cu^{2+} > Zn^{2+} > Cd^{2+}$. The dynamic adsorption of the column depends on the flow rate, bed height, initial metal concentration, and SDS surface modification. With a 5 mL/min flow rate, a 20 cm bed height, and a 50 mg/L initial metal concentration, a maximum break-through time of 150 minutes for the unmodified activated carbon (AC) and 180 minutes for the SDS-modified activated carbon (AC-SDS) was reached.

Keywords

Adsorption, Surfactant-Modified Activated Carbon, Multicomponent, Breakthrough, Adsorption Capacity, Fixed Bed Column

1. Introduction

The discharge of untreated sewage and industrial effluent containing heavy metals into water bodies has resulted in various health and environmental issues and a reduction in the quantity and quality of freshwater available for domestic, agricultural, and industrial purposes [1]-[3]. Conventional wastewater treatment technologies such as ion-exchange, chemical precipitation, evaporation, membrane separation, electrochemical treatment, and reverse osmosis have limitations including lack of specificity and inefficiency at low concentrations, membrane fouling caused by slightly soluble components, large footprint requirements, sludge dewatering facilities, the need for highly skilled operators, and high costs [1] [3]-[5]. Consequently, there is a need for a cost-effective and efficient water treatment technology that can be readily scaled up for commercial production [4] [6].

Adsorption using activated carbon could be used as an alternative wastewater treatment technique because it is easier to install, requires less operation and maintenance costs, and is available as a cheap adsorbent [7]. The most preferred one is granular activated carbon adsorption. Unlike powdered activated carbons, granular activated carbons possess superior mechanical qualities and can be easily separated from treated water due to their larger and harder nature [7] [8]. However, compared to powdered activated carbon, the adsorption capacity of granular activated carbon for heavy metals is relatively lower due to the fewer active binding sites (surface functional groups) for such contaminants.

Activated carbon's capacity to adsorb cations has been improved through the use of numerous functional and surface modification techniques. These consist of surface modification [9]-[12] and chemical or physical treatment [13]-[15]. The surfactant surface modification (impregnation) method is one of the techniques that significantly increase activated carbons' capacity to adsorb heavy metals including chromium, cadmium, and zinc [16]-[18].

Furthermore, in batch studies [18] [19] and fixed column study [20], the incorporation of surfactant to the surface of activated carbons has been reported to exhibit higher adsorption capacities than unmodified ones for the adsorption of a single solution of cationic heavy metals; however, the actual wastewater is typically a mixture of multiple metals. Competitive adsorptions of multiple heavy metals onto surfactant-modified activated carbon in a fixed or expanded column have not been widely studied.

The aim of this work is to examine the capacity of both unmodified and modified activated carbon with sodium dodecyl sulfate (SDS) to adsorb Pb^{2+}, Cu^{2+}, Zn^{2+}, and Cd^{2+} simultaneously from an aqueous solution. FT-IR, SEM, and BET surface area analyzers were used to characterize the adsorbents. The dynamics of the fixed bed column were investigated in relation to flow velocity, bed height, and initial metal concentration.

2. Materials and Method

2.1. Materials

The chemicals used in this study were of analytical grade. Sulphuric acid, H_2SO_4

(>99%), phosphoric acid, H_3PO_4 (>99%), sodium hydroxide solution, NaOH (>99%), $Pb(NO_3)_2$, $CuSO_4{\cdot}5H_2O$, lead (II) nitrate, $Pb(NO_3)_2$ (99.5%), copper sulfate pentahydrate, $CuSO_4{\cdot}5H_2O$ (99.5%), zinc (II) sulfate heptahydrate, $ZnSO_4{\cdot}7H_2O$ (99.5%), cadmium chloride monohydrate, $CdCl_2{\cdot}H_2O$ (99.5%), sodium dodecyl sulphate (SDS), Whatman® filter papers, distilled water were obtained from Advanced Organic Laboratory, SHESTCO, Sheda, Kwali, Abuja, Nigeria.

2.2. Collection and Preparation of Coconut Shell

The carbon adsorbents were made using coconut shells that were procured from a local vendor at Ibrahim Badamosi Babangida Market in Suleja, Niger State, Nigeria. To get rid of any contaminants, the coconut shells were carefully cleaned with distilled water. Then it was sun-dried for 8 - 10 hours to promote crushing and grinding. The dried coconut shells were crushed using a hand crusher, while a grinding machine was used to turn them into a fine powder. An electronic sieve was used to filter the resulting ground powder, and only powder with a particle size of less than 150 m was chosen to be used in the creation of the activated charcoal.

2.3. Physicochemical Analysis of the Produced Activated Carbon

The physicochemical analyses of the activated carbon produced were conducted to determine its properties like BET surface area, pore volume, ash content, moisture content, volatile content and fixed carbon as listed in Table 1.

Table 1. Physicochemical properties of the activated carbon produced.

S/N	Properties	Activated carbon (AC)
1	BET surface area	1410 m^2/g
2	Pore volume	0.715 cm^3/g
3	Ash Content	5 wt%
4	Moisture content	8 wt%
5	Volatile matter	13 wt%
6	Fixed carbon	74 wt%

2.4. Preparation of Adsorbent

Adsorbent was prepared by chemical carbonization of the coconut shell. A phosphoric acid aqueous solution (98% m/m) was prepared in the volumetric ratio 63:37, phosphoric acid: water [21] [22]. This mixture was thoroughly mixed in a 40/60 (mass/volume) ratio with coconut shells feedstock and it was allowed to undergo drying overnight at 45˚C. The hydrolytic solid was pyrolyzed at 350˚C for 30 min followed by an increase of temperature to 480˚C for an additional 1 h to produce carbon char. The resulting char was then washed with distilled water containing 0.15% formic acid and then washed severally with distilled water [1] [23]. The resulting mixture was filtered using Whatman filter paper (pore size:

0.45 μm) until free of activator as indicated by silver nitrate test. Finally, the charcoal was dried at 110˚C for 2 h and then weighed to determine the activated carbon yield. The solid obtained was designated as activated carbon (AC) and then stored in plastic bottles to prevent adsorption of dust, moisture and other particles from the atmosphere [3] [24]. The percentage yield was calculated using Equation (1).

$$\text{Percentage yield} = \frac{Wa}{Wp} \times 100\% \quad (1)$$

where:

Wa is the mass of activated charcoal and Wp is the mass of precursor.

2.5. Modification with Surfactant

A 10.1 g of SDS was dissolved in 1000 mL of distilled water to produce 10 g/L of standard SDS solution. Subsequent lower SDS concentration was prepared by the diluting standard SDS solution. Modification was carried out by treating, 5 g of adsorbent (AC) with 100 mL solution of anionic surfactant at 1.5 mol/L correspond to 1.5 Critical Micelle Concentrations (CMC). This 1.5 CMC was selected to maximize the amount of surfactant adsorbed onto the AC. The sample was placed and allowed to agitate in a temperature controlled orbital shaker at 160 rpm, for 6 hr. The sample was filtered by Whatman filter paper (0.42 μm) without rinsing and then dried in an oven overnight at 110˚C [18] [25]. Finally, SDS modified AC obtained and labelled as AC-SDS. SDS was selected amongst others for this research work due to its low cost, availability and effectiveness [25] [26].

2.6. Determination of the Point of Zero Surface Charge of the Adsorbents

The point of zero surface charge (pH_{PZC}) for the adsorbents was calculated using the procedure outlined by Kandah *et al.* [27]. 100 mL of a 0.01 M KNO_3 solution was placed in five conical flasks with a capacity of 250 mL each. The initial pH of the solutions in the flasks was adjusted to 2, 4, 6, 8, and 10 by adding appropriate amounts of 0.1 M HCl or 0.1 M NaOH solutions. Subsequently, 0.2 g of the specified adsorbent was introduced into each flask and agitated for 48 hours at 30˚C. The final pH of the mixture was measured and recorded after 48 hours using a pH meter. The difference between initial and final pH ($\Delta pH = pHi - pH_f$) values was calculated. ΔpH was plotted against the corresponding pHi, as shown in Figure. The pH_{PZC} for AC and AC-SDS were read off from the plot at a ΔpH of zero.

2.7. Characterization of the Adsorbents and Metal Solutions

For the determination of specific surface area and pore volume of the carbonized coconut shell without activation (CCS), activated carbon (AC) and surfactant-modified carbon (AC-SDS), the Brunauer-Emmett-Teller (BET) method was adopted and for that purpose, a Micrometrics automatic surface area analyzer (Gemini 2360, Shimadzu, Japan) was used. The concentrations of the lead, copper,

zinc and cadmium ions in the synthetic multiple metal solutions adsorption were determined by using an atomic adsorption spectrophotometer (Perkin Elmer Model AAS 700). A portable pH meter (Hach) was used to determine the solution's pH. The surface functional groups of the adsorbent were identified by the Fourier transform infrared spectroscopy (FTIR) (Bruker 3000 Hyperion, Germany). Morphological analysis of the adsorbent was done by using the scanning electron microscope (SEM) (JELO JSM7600F) supported by EDXS (energy dispersive X-ray spectroscopy) (Oxford Aztec energy system).

2.8. Preparation of the Stock Solution and Synthetic Wastewater

Aqueous solution of synthetic multicomponent metal ions was used throughout this study to represent a simple model of effluent containing heavy metals (Lead-Pb, Copper-Cu, Zinc-Zn, and Cadmium-Cd). The stock solution of 1000 mg/L was prepared for each metal ion (Pb^{2+}, Cu^{2+}, Zn^{2+}, and Cd^{2+} ions) through the dissolution of an appropriate amount of the respective salt. Thus, for Pb: 1.60 g of lead (II) nitrate, Pb $(NO_3)_2$, for Cu: 3.90 g of copper sulfate pentahydrate, $CuSO_4{\cdot}5H_2O$, for Zn: 4.44 g of zinc (II) sulfate heptahydrate, $ZnSO_4{\cdot}7H_2O$, and for Cd: 1.80 g of cadmium chloride monohydrate, $CdCl_2$. Each salt was weighed out, dissolved in deionized water, and made up to a final volume of 1.0 liters. The stock solutions were further diluted as per the required concentrations using Equation (2) and labeled as simulated wastewater (SWW-Pb, SWW-Cu, SWW-Zn, and SWW-Cd).

$$C_1V_1 = C_2V_2 \tag{2}$$

where: C_1 is the concentration of the stock solution, V_1 is the volume of stock required to make the expected working solution, C_2 is the expected concentration of working solution and V_2 is the volume of the working solution.

For Zn, 4.44 g of zinc (II) sulfate heptahydrate, $ZnSO_4{\cdot}7H_2O$, was arrived at as follows:

Molecular mass of $ZnSO_4{\cdot}7H_2O$ = 65 + 32 + (4 × 16) + 7 (2 × 1 + 16) = 287 g

Mass of Zn in $ZnSO_4{\cdot}7H_2O$ = 65 g

The mass of $ZnSO_4{\cdot}7H_2O$ to be dissolved in 1000 mL of distilled water to produce 1000 mg/L of Zn stock solution is 287/65 = 4.415 g/0.995 (99.5% purity) = approximately 4.44 g. The same procedure was used for Pb, Cu, and Cd.

2.9. Preparation of Mixed-Metal Ions Solution

All the chemicals used for these experiments were sourced from Advanced Organic Chemistry Laboratory, SHESTCO, Sheda, Kwali, FCT, Abuja, and ensured that they were of analytical grade. In a multicomponent solution, the concentration of each component in the mixture was the same by adding an equal volume of 1000 mL each of the four metal ion stock solution prepared as outlined in Section 2.8, which means that the final concentration of each of the cations in the solution was 250 mg/L. The mixture was further diluted to a desired concentration

using Equation (2) and designated as simulated wastewater (SWW). The final concentrations of each metal in the mixed metal solution after the adsorption experiment were determined using an atomic absorption spectrometer (AAS).

2.10. The Column Experiments

The experimental set-up for continuous study was similar to Patel's [2], as shown in Figure 1. The column was made up of glass with a 300-mm high and 21-mm internal diameter. For a consistent flow of mixed metal solution and to avoid channeling, a glass bead layer 2 cm high was placed at the bottom of the column. After the glass bead, four sampling points at intervals of 5 cm were situated on the column's wall for convenient collection of samples. A mixed metal solution was fed at specified flow rate through a peristaltic pump into the column using bottom-to-top mode [2]. Glass wool was placed on the bottom and top of the column to keep the adsorbents in place. The residual concentration of lead, copper, zinc, and cadmium in the outlet stream from the adsorbent column setup was sampled and analyzed at regular intervals (30 minutes) of 50 mL of effluent volume using the atomic absorption spectrometer (AAS) machine [2] [3].

Prior to loading of the adsorbents in the column, the adsorbents were soaked in distilled water, washed and decanted 4 times, to remove fine particles from causing pressure drop in the column. The adsorbents after drying at 110˚C, were then packed in the column to a known height depending on the column parameter varied at a point in time, then filled with distilled water and kept submerged before loading the column with the pollutant, to avoid air entrapment in the bed and prevent channeling that would lower bed utilization as explained by Goel *et al.* [1].

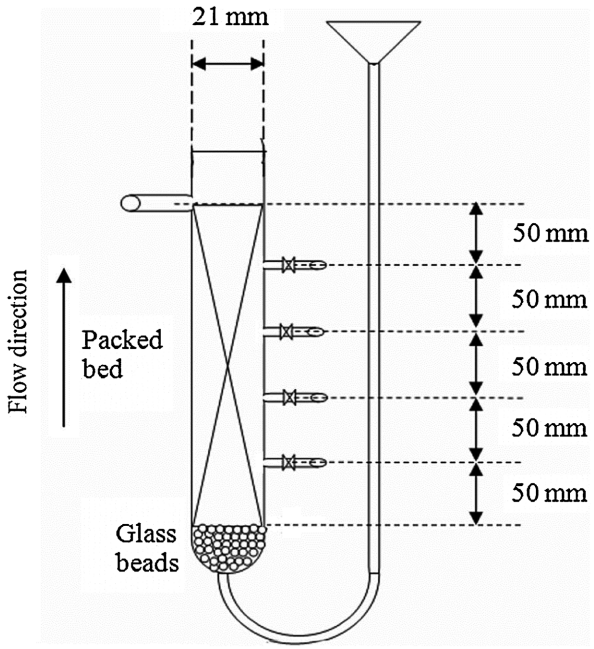

Figure 1. Schematic diagram of the column used in the adsorption study, Source [2].

2.10.1. Effect of Flow Rate (Q)

The flow rates were varied at 5, 10, and 15 mL/min to examine its effect on the amount of heavy metal adsorbed by the AC or AC-SDS. The bed height and inlet concentration were kept constant at 20 cm and 250 mg/L, respectively.

2.10.2. Effect of Bed Height (Z)

The bed heights were varied at 10, 15, and 20 cm to examine its effect on the amount of heavy metal adsorbed by the AC or AC-SDS. The flow rate and inlet concentration were kept constant at 5 mL/min and 250 mg/L, respectively.

2.10.3. Effect of Initial Inlet Concentration (C_o)

The initial inlet concentrations were varied at 50, 150, and 250 mg/L to examine its effect on the amount of heavy metal adsorbed by the AC or AC-SDS. The bed height and flow rate were kept constant at 20 cm and 5 mL/min, respectively.

2.11. Parameters of the Breakthrough Curve

The residual metal concentration in the outlet stream of the AC and AC-SDS expanded bed were used to plot the breakthrough curve by plotting fractional ratio, equation (3) against adsorption time (min) [28].

$$f = \frac{C_t}{C_o} \tag{3}$$

where C_t is the residual metal concentration the outlet stream and C_o is the concentration of the metal in the feed solution. The breakthrough parameters and the formula for its determination are listed in Table 2.

Table 2. Breakthrough parameters, Patel [2] with little modifications

S/N	Breakthrough parameters	Formula	Reference
1.	Breakthrough time (t_b)	Time at $f = \frac{C_t}{C_o} = 0.1$	[2]
2.	Exhaust time (t_e)	Time at $\frac{C_t}{C_o} = 0.9$	[2]
3.	Breakthrough volume (V_b)	$V_b = t_b \times \text{Flow rate}(Q)$	[2]
4.	Exhaust volume (V_e)	$V_e = t_e \times \text{Flow rate}(Q)$	[2]
5.	Mass transfer zone moving time (t_δ)	$t_\delta = \frac{V_e - V_b}{\text{Flow rate}}$	[2]
6.	Adsorption capacity at ($t_{0.5}$) (mg/g)	$q_e @ t_{0.5} = \frac{t_{0.5} Q C_o}{m}$	[2]
7.	Height of MTZ (H_{MTZ})	$H_{MTZ} = \frac{Z(t_e - t_b)}{t_e}$	[2]
8.	MTZ moving rate (U_Z)	$U_Z = \frac{H_{MTZ}}{t_\delta}$	[2]

3. Results and Discussion

3.1. Characterization of the Coconut Shell and the Adsorbents

Scanning Electron Microscopy (SEM)

The characterization of the raw coconut shell (RCS), the carbonized coconut shell (CCS), the activated carbon before adsorption (ACB), the surfactant modified activated carbon before adsorption (AC-SDSB), activated carbon after adsorption (ACA), and the surfactant modified activated carbon after adsorption (AC-SDSA) was studied using SEM micro grip has shown in Figures 2(a)-(f) respectively. The SEM image enables the direct observation of the changes in the surface microstructures of the carbons due to the modifications as well as the morphology character of the coconut shell. Figure 2(a) (RCS) shows a rough surface with visible pores and irregular shapes and Figure 2(b) (CCS) shows a smoother surface with fewer visible pores, indicating that the coconut shell has been treated at high temperature resulting in a reduction in its surface area.

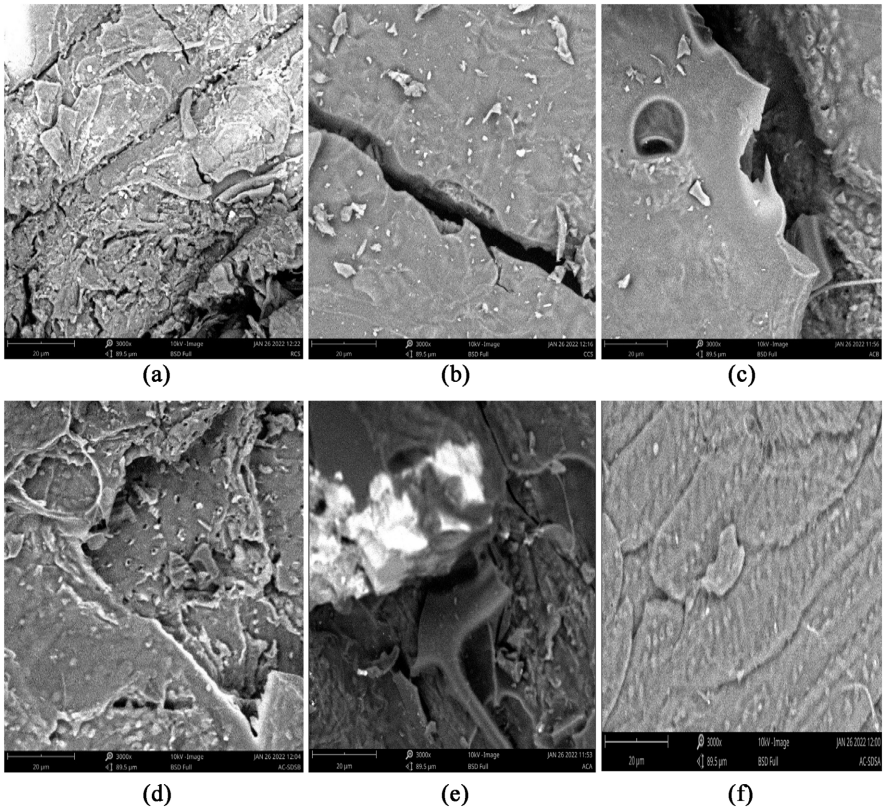

Figure 2. SEM Analysis of (a) Raw Coconut shell (RCS); (b) Carbonized coconut shell (CCS); (c) Activated carbon before adsorption (ACB); (d) SDS-modified activated carbon before adsorption (AC-SDSB); (e) Activated carbon after adsorption (ACA) and (f) SDS-modified Activated carbon after adsorption (AC-SDSA).

Figure 2(c) (ACB) shows a highly porous structure with small pores and a large surface area, which is ideal for adsorption and these pores are filled by Pb^{2+}, Cu^{2+}, Zn^{2+}, and/or Cd^{2+} observed in Figure 2(e) (ACA). In Figure 2(d) (AC-SDSB),

there is obvious demarcation in the surface morphology of (ACB) after treatment with surfactant which shows a modified surface structure, which has been treated with SDS surfactant resulting in a smoother and more uniform surface and these surfaces are filled by metal ions as depicted in Figure 2(f) (AC-SDSA). This modification is intended to increase the net surface charge of the activated carbon to negative for efficient removal of the positive heavy metal ions from the aqueous media.

3.2. Fourier Transform Infrared Spectroscopy (FT-IR) Analyses for Samples

The FTIR spectra of RCS, CCS, AC and AC-SDS before and after adsorption of metal ions were analyzed in the range of 650 - 4000 cm^{-1}, and different functional groups on their surfaces were assigned to the observed peaks (Table 3 and Table 4). The results revealed absorption peaks corresponding to various functional groups or vibration modes, including O–H and N–H bonds stretching, C=O bond

Table 3. FTIR band assigned to the produced samples before the adsorption process.

Frequency (cm^{-1})	Functional group/Assignment	Observed frequency (cm^{-1})			
		RCS	CCS	ACB	AC-SDSB
4000 - 3500	Alcohols (O-H stretch)			3906.25	
3499 - 3000 900 - 650	Amines, amides (N-H stretch)	3287.51 764.10, 853.56	 868.46 - 749.19	3287.51, 3138.41 890.83 - 738.01	3280.05 - 3019.14 872.19 - 693.28
2700 - 2500 2499 - 2000 1320 - 1210	Carboxylic acids (O-H stretch)	2370.58 - 2117.12	 1241.20	 2374.31, 2325.85 1230.02	2657.59 2374.31, 2322.13
		Carbonyls			
1650 - 1600	Ketones (C=O stretch)	1636.30			
2800 - 2700 1740 - 1725	Aldehydes (C=O stretch)				1736.93
1750 - 1700	Esters (C=O stretch)				
1610 - 1550 1420 - 1300	Carboxylic acid (C=O stretch)	 1330.65, 1420.11	 1561.75	1558.02 1394.02	1561.75 1364.20
		Aliphatic groups			
2970 - 2950 2880 - 2860 1470 - 1430	Alkenes (=-CH_3 stretch)	2922.23 1457.38		 1457.38	
1600 - 1500	Alkenes (C=C stretch)	1509.57			
770 - 730	Alkyne (-C-H stretch)	764.10	749.19	738.01	745.46
		Sulfonyl group			
700 - 900 1350 - 1450	Sulfonate (S–O–C) Sulfone (S=O)				1353.02 - 1449.83 700.73 - 898.28

Table 4. FTIR band assigned to the produced samples after adsorption processes.

Frequency (cm^{-1})	Functional group/Assignment	Observed frequency (cm^{-1})	
		ACA	AC-SDSA
4000 - 3500	Alcohols (O-H stretch)		3947.25 - 3585.69
3499 - 3000 900 - 650	Amines, amides (N-H stretch)	3403.05, 3302.42 875.92 - 689.55	3321.05, 3026.59 872.19 - 745.46
2700 - 2500 2499 - 2000 1320 - 1210	Carboxylic acids (O-H stretch)		2370.58, 2340.76 1215.11
	Carbonyls		
2800 - 2700 1740 - 1725	Aldehydes (C=O stretch)		2780.59
1750 - 1700	Esters (C=O stretch)		1699.66
1610 - 1550 1420 - 1300	Carboxylic acid (C=O stretch)	1558.02 1420.11, 1364.20	1558.02 1364.20
	Aliphatic groups		
2970 - 2950 2880 - 2860 1470 - 1430	Alkenes (=-CH_3 stretch)		2877.50 1457.38
770 - 730	Alkyne (-C-H stretch)	752.92	745.46

stretching, and –COOH groups are on the surfaces of the samples. These carboxylic, carbonylic and phenolic acid groups are known to create adsorbent surface charge that favours metal adsorption. For activated carbon before adsorption (ACB)'s spectra (**Figure 3**), the broad bonds at 3138.41 cm^{-1}, 3287.51 $cm^{-1}$and 3906.25 cm^{-1} were assigned to O–H and N–H bonds stretching [22] [29]. The absorption peaks at 1394.02 cm^{-1} and 1558.02 cm^{-1}were assigned to stretching vibration of C=O bond. The bounds observed in the range of 2325.85 cm^{-1} and 2374.31 cm^{-1} indicated the presence of –COOH groups on ACB surface [2] [25]. These carboxylic, carbonylic and phenolic acid groups noticed on the RCS, CCS, AC and AC-SDS have been reported in literatures to cause adsorbent surface charge which favours metal adsorption [1] [4] (Goel *et al.*, 2005; Fatimah *et al.*, 2017). In addition, the absorption peaks at 1457.38 cm^{-1} and 1129.38 cm^{-1} were corresponded to N–O bond and C–O bond, respectively [1] [25] [30].

Almost all peaks found on ACB were also observed with little shifts on the spectrum of AC-SDSB before metal ions adsorption, as shown in **Figure 4**. However, some other peaks appeared in the spectrum of AC-SDSB when it was modified with SDS. The absorption bonds at wave number values ~2657.59 cm^{-1} and ~1736.93 cm^{-1} were attributed to $-CH_2$ and C=C bonds, respectively. Herein, $-CH_2-$ group is due to the alkane groups which comes from SDS [25] [31]. In addition, the peaks at around 1350 - 1450 cm^{-1} and 700 - 900 cm^{-1} were attributed to the S=O (Sulfone or sulfonyl group) and S–O–C (sulfonate or sulfonic acid ester

group) bonds, respectively which were from polar head group of SDS [25]. These results clearly indicated that SDS was successfully incorporated into the AC structure [6] [26].

For AC-SDSA after metal ion adsorption (**Figure 4**), functional groups such as $-CH_2$ (1699.66 cm^{-1}), N–O (1457.38 cm–1) and C–O (1032.47 cm^{-1}) were affected by metal ions adsorption. Furthermore, the intensity absorption of the peak of 745.46 cm^{-1} which was assigned to the C–H bond was reduced remarkably after the adsorption of metal ions [31]. As can be seen in **Figure 4**, the absorption peaks belonged to S=O and S–O–C bonds did not appear in the AC-SDSA spectra after adsorption process. This conforms to what was reported in the previous researches [25] [31]. When compared to the spectrum of activated carbon after the adsorption (ACA), the absorption peak at 1215.11 cm^{-1} (attributed to C–O bond) was broader after metal ion adsorption, indicating that the adsorption of metal ions onto the AC's surface was affected by these functional groups as presented in **Table 4**.

The carboxyl and lactone functional groups improve the ion exchange properties of adsorbents [31]. The carbonyl, hydroxyl, carboxyl and amino functional groups which were confirmed to be present on the surface of both unmodified activated and SDS-modified activated carbon in the current study act as binding sites for the positively charged heavy metals in the aqueous medium. In addition, the SDS-modified activated carbon contain S=O and S–O–C sulfonyl functional groups which could provide enhanced adsorption capacity for the heavy metals.

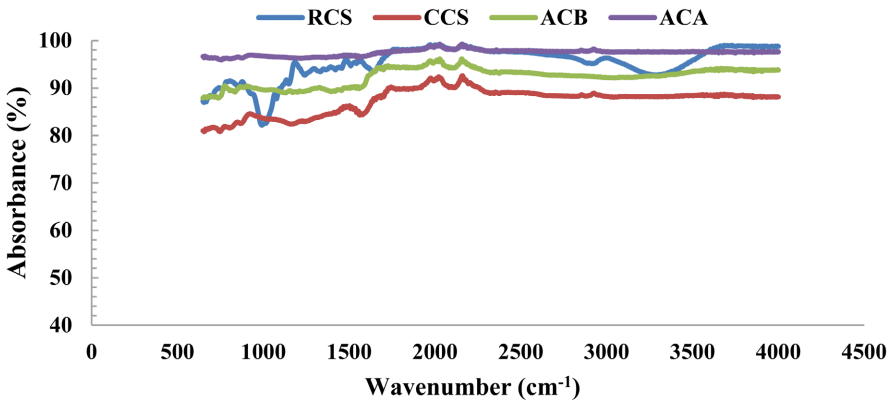

Figure 3. FT-IR spectra of raw coconut shell (RCS), carbonized coconut shell (CCS), H_3PO_4-activated carbon before adsorption (ACB) and after adsorption (ACA).

Figure 3 compares the FTIR spectra of raw coconut shell (RCS), carbonized coconut shell (CCS), and H_3PO_4-activated carbon before adsorption (ACB). The broad peak at around 3500 cm^{-1} in all three spectra is due to the O-H stretching of adsorbed water molecules. The peak at around 2920 cm^{-1} corresponds to the C-H stretching vibration in the carbon materials. The presence of the peak at around 1720 cm^{-1} in the CCS and ACB spectra indicates the presence of carbonyl groups in the samples. The carbonyl peak is absent in the RCS spectrum. The peaks at around 1600 cm^{-1} and 1400 cm^{-1} correspond to the C=C and C-H

bending vibrations, respectively, and are more pronounced in the CCS and ACB spectra.

Figure 3 shows the FTIR spectra of CCS, H_3PO_4-activated carbon before adsorption (ACB), and after adsorption (ACA). The spectrum of ACA shows a decrease in intensity of the peaks at around 1720 cm^{-1}, indicating the removal of carbonyl groups upon adsorption. The peak at around 3420 cm^{-1} in the ACA spectrum corresponds to the O-H stretching vibration of surface hydroxyl groups, indicating the presence of surface functional groups due to adsorption.

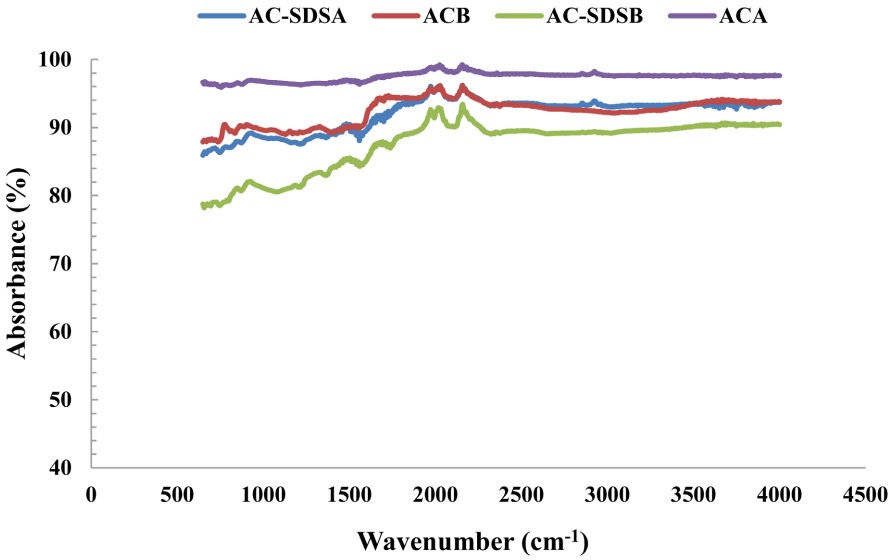

Figure 4. FT-IR spectra of H_3PO_4-activated carbon before adsorption (ACB), H_3PO_4-activated carbon after adsorption (ACA), surfactant-modified AC before (AC-SDSB) and after adsorption (AC-SDSA).

Figure 4 shows the FTIR spectra of H_3PO_4-activated carbon before (ACB) and after adsorption (ACA), surfactant-modified AC before (AC-SDSB) and after adsorption (AC-SDSA). The spectra of AC-SDSB and AC-SDSA show a new peak at around 2850 cm^{-1}, which corresponds to the C-H stretching vibration in the surfactant molecule. This peak is absent in the ACB spectrum, indicating the successful modification of the activated carbon with the surfactant. The peak at around 3420 cm^{-1} in the AC-SDSA spectrum indicates the presence of surface hydroxyl groups due to adsorption.

3.3. Net Surface Charge of the Activated (AC) and Modified Activated (A-SDS) Carbons

Figure 5 shows the net surface charge of the AC and AC-SDS as the initial pH of the solution varied from 2 to 10. The figure clearly shows that the net surface charge for both adsorbents changed from positive to negative as the pH increased. The net surface charge on the AC-SDS became zero at a pH of 5.4, while that of the AC attained zero at a pH of 5.6. Each adsorbent's net surface charge increases after reaching pHpzc, or the point of zero surface charge. SDS was bonded to the

surface of the modified activated carbon, thus the net negative surface charge of AC-SDS was always greater than that of AC. Additionally, prior studies have demonstrated that anionic surfactant modification increases the net negative surface charge of virgin activated carbons, and as pH rises, the net negative surface charge of these carbons increases [6] [18] [25]. More binding sites are available to adsorb more positively charged heavy metals, such as Pb^{2+}, Cu^{2+}, Zn^{2+}, and Cd^{2+} when there is an increase in the net negative surface charge on the activated carbons. This is why in this current study the modified activated carbon, AC-SDS, exhibits greater adsorption capacity for all the four heavy metals (Pb^{2+}, Cu^{2+}, Zn^{2+}, and Cd^{2+}) than the unmodified activated carbon, AC.

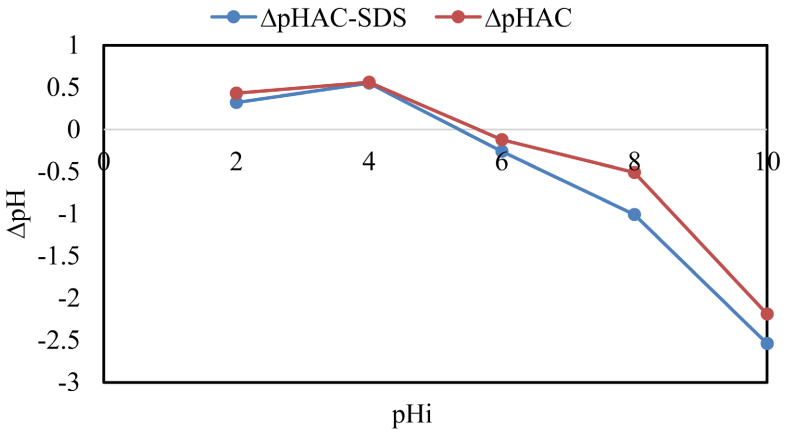

Figure 5. Plot of net surface charge of the adsorbents versus initial pH.

3.4. Column Performance

Figures 6-14 show the concentration of each metal ion in the outlet stream plotted against the adsorption time. The illustrations depict the characteristic "S" form of a breakthrough curve; however, the breakthrough time, steepness, and exhaust (saturation) time differ for Pb^{2+}, Cu^{2+}, Zn^{2+}, and Cd^{2+} ions individually. The surface modification of the activated carbon by the SDS surfactant, flow rate, bed height, and initial metal concentration are the main causes of these differences.

3.4.1. Effect of Flow Rate on the Adsorption of the Heavy Metal Ions

Figure 6 shows the outlet heavy metal concentration against the adsorption time for 5 mL/min flow rate. For the unmodified activated carbon (AC), Cd^{2+} has the least affinity with 22.1% of its initial concentration appears in the outlet stream in 60 min, followed by 11% of initial Zn^{2+} shows up in 60 min, 14.4% of initial Cu^{2+} appears in 90 min, while Pb^{2+} exhibits the highest affinity for the adsorbent, with 13.2% of its initial concentration shows up in the outlet stream in 120 min.

Similarly, Cd^{2+} exhibits the lowest affinity for the adsorbent when it comes to the modified activated carbon (AC-SDS); 10.5% of its initial concentration shows up in 60 minutes, followed by 15.4% of initial Zn^{2+} appears in 120 minutes, 13.9% of initial Cu^{2+} appears in 120 minutes, and 15% of initial Pb^{2+} shows up in 150 minutes, making it have the highest affinity for the AC-SDS. In AC-SDS, as

opposed to AC, every metal displayed a greater break-through time, which indicates a higher adsorption capacity than AC. This is because the AC has additional binding sites for the adsorption of heavy metals as a result of the incorporation of SDS into it.

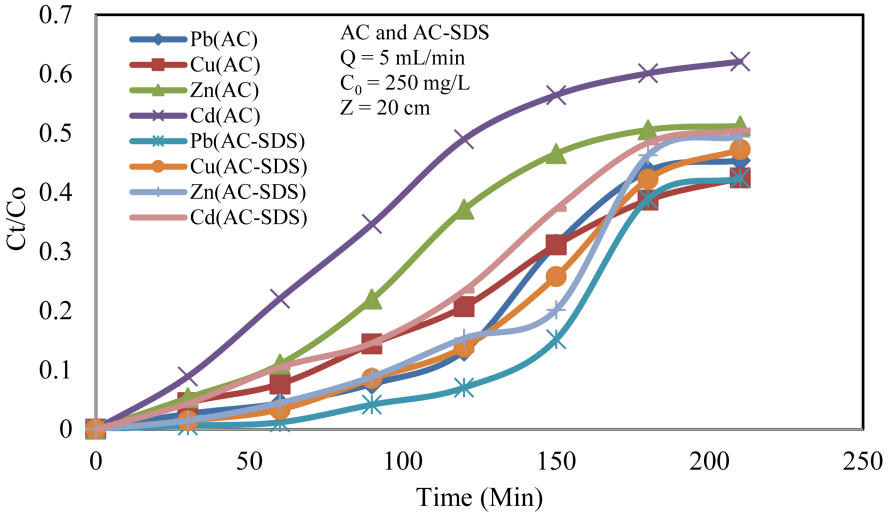

Figure 6. Breakthrough curves for simultaneous adsorption of heavy metals (Pb, Cu, Zn and Cd) onto AC and AC-SDS: Effect of flowrate (Q = 5 mL/min; C_0 = 250 mg/L, Z = 20 cm).

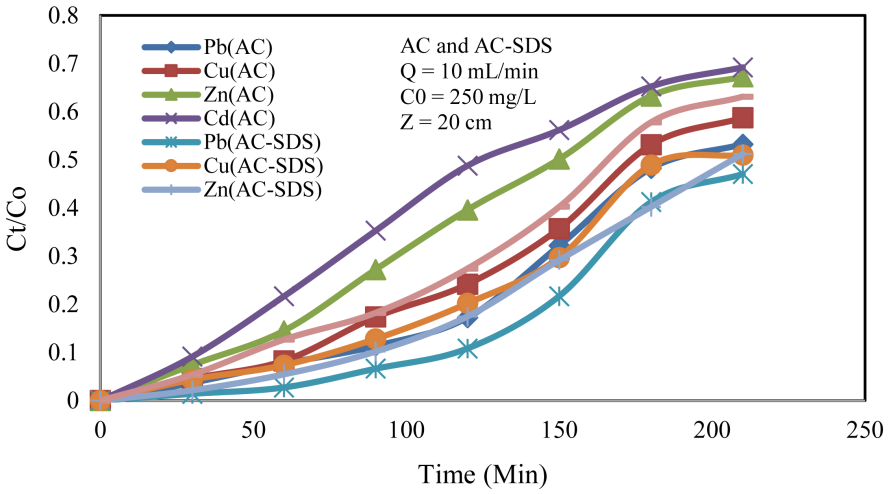

Figure 7. Breakthrough curves for simultaneous adsorption of heavy metals (Pb, Cu, Zn and Cd) onto AC and AC-SDS: Effect of flowrate (Q = 10 mL/min; C_0 = 250 mg/L, Z = 20 cm).

Figure 7 shows the outlet heavy metal concentration against the adsorption time for 10mL /min flow rate. For the AC, Cd^{2+} has the least affinity with 21.7% of its initial concentration appears in the outlet stream in 60 minutes, followed by 14.5% of initial Zn^{2+} concentration shows up in 60 minutes, 17.3% of initial Cu^{2+} appears in 90 minutes, while Pb^{2+} exhibits the highest affinity for the adsorbent, with 11.4% of its initial concentration shows up in the outlet stream in 90 minutes.

In addition, Cd^{2+} exhibits the lowest affinity for the adsorbent when it comes to the SDS-AC; the outlet stream contains 12.7% of its initial concentration in 60minutes, 10.2% of initial Zn^{2+} in 90 minutes, 12.8% of initial Cu^{2+} in 90 minutes, and 10.8% of initial Pb^{2+} in 120 minutes, making it have the highest affinity for the AC-SDS. Every metal displayed a greater breakthrough time in AC-SDS than AC. This is because the AC has additional binding sites for the adsorption of heavy metals as a result of the incorporation of SDS into AC.

Figure 8 shows the outlet heavy metal concentration against the adsorption time for 15 mL/min flow rate. For the AC, in 30 minutes, 18.2% of initial Zn^{2+} concentration, 14% of initial Cd^{2+} concentration, and 10.9% of initial Cu^{2+} concentration shows up in 30 min, while 20.3% of initial Pb^{2+} concentration appears in the outlet stream. This shows Zn^{2+} has the least affinity for the adsorbent followed by Cd^{2+} and Cu^{2+} and Pb^{2+} exhibits the highest affinity for the adsorbent.

For the AC-SDS adsorbent, Cd^{2+} exhibits the lowest affinity, with 12.3% of its initial concentration showing up in 30 minutes, followed by 10.6% of initial Zn^{2+} appearing in 30 minutes, 16% of initial Cu^{2+}, and 12.2% of initial Pb^{2+} appearing in 60 minutes, making Pb^{2+} have the highest affinity for the AC-SDS. In AC-SDS, as opposed to AC, every metal displayed a greater break time. This is because the AC-SDS has more binding sites for the adsorption of heavy metals due to the incorporation of SDS into the AC.

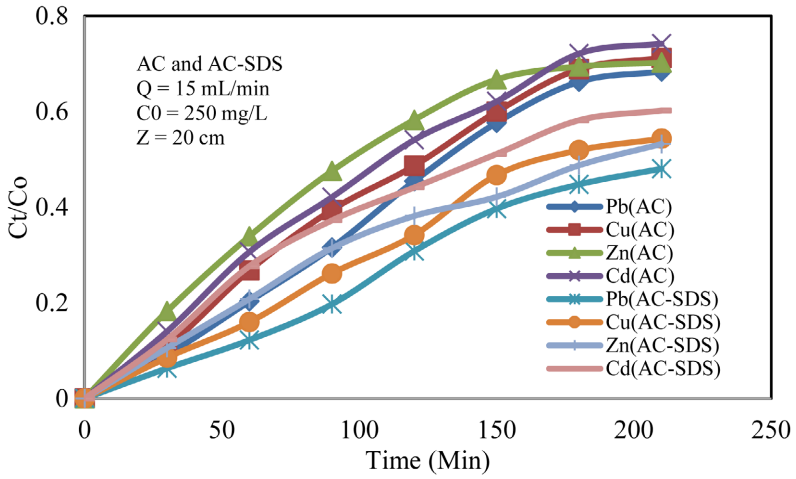

Figure 8. Breakthrough curves for simultaneous adsorption of heavy metals (Pb, Cu, Zn and Cd) onto AC and AC-SDS: Effect of flowrate (Q = 15 mL/min; C_0 = 250 mg/L, Z = 20 cm).

As shown in Figures 6-8, an increase in flow rates from 5 to 15 mL/min generally reduces the breakthrough time in both AC and SDS-AC for all the metals. Compared to the AC-SDS, the breakthrough time of the AC is lower. This is explained by the incorporation of SDS on the AC, which gives the heavy metals additional binding sites. A rise in flow rate caused an increase in the amount of metals adsorbed onto the unit bed height (mass-transfer zone), which accelerated saturation [32]. At a lower flow rate, adsorbate has more time to contact the

adsorbent, which results in a higher removal of adsorbate from the column [33] [34].

3.4.2. Effect of Bed Height on the Adsorption of the Heavy Metal Ions

Figure 9 shows the outlet heavy metal concentration against the adsorption time for a 10 cm bed height. For the AC, in 30 minutes, 27.4% of the initial Cd^{2+} concentration, 24.3% of the initial Zn^{2+} concentration, 20.1% of the initial Cu^{2+} concentration, and 16.9% of the initial Pb^{2+} concentration appear in the outlet stream. That indicates that, in terms of affinity for the adsorbent, Pb^{2+} has the highest, followed by Cu^{2+} and Zn^{2+}, while Cd^{2+} has the lowest.

Similarly, for the AC-SDS, in 30 minutes, 19.7% of the initial Zn^{2+} concentration, 18.9% of the initial Cd^{2+} concentration, 16.7% of the initial Cu^{2+} concentration, and 13.3% of the initial Pb^{2+} concentration appear in the outlet stream. That means, with regard to affinity for the adsorbent, Pb^{2+} has the highest, followed by Cu^{2+} and Cd^{2+}, while Zn^{2+} has the lowest. Again in AC-SDS as opposed to AC, every metal displayed a greater breakpoint. This is because the AC-SDS has more binding sites for the adsorption of heavy metals as a result of the incorporation of SDS on it on the AC.

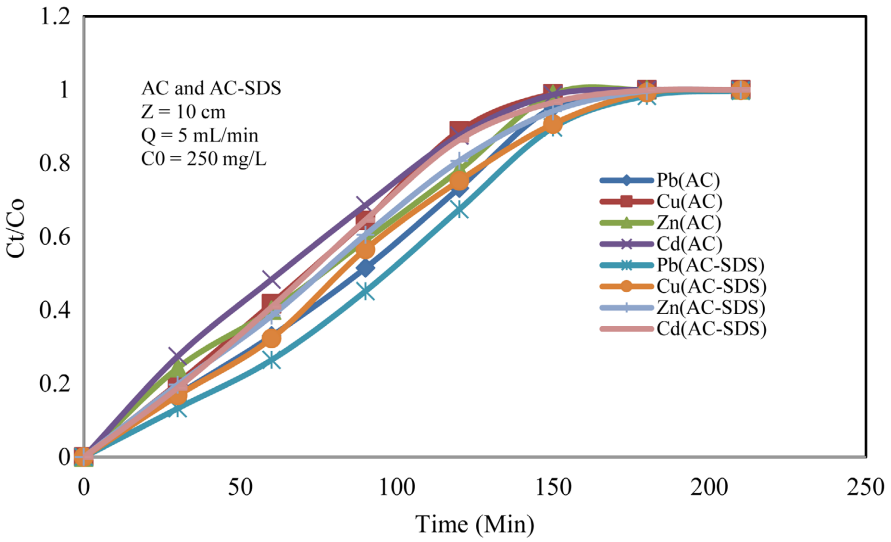

Figure 9. Breakthrough curve for simultaneous adsorption of heavy metals (Pb, Cu, Zn and Cd) onto AC and AC-SDS: Effect of bed height (Q = 5 mL/min; C_0 = 250 mg/L, Z = 10 cm).

Figure 10 shows the outlet heavy metal concentration against the adsorption time for a 15 cm bed height. For the AC, in 60 minutes, 10.2% of the initial Pb^{2+} concentration, 16.7% of the initial Cu^{2+} concentration, and 18.9% of the initial Zn^{2+} concentration appear in the outlet stream. In 30 minutes, 10.9 of the initial Cd^{2+} concentration appear in the outlet stream. With regard to affinity for the adsorbent, Pb^{2+} has the highest, followed by Cu^{2+} and Zn^{2+}, while Cd^{2+} has the lowest.

Similarly, for the AC-SDS, the outlet stream contains 14.2% of the initial Pb^{2+} concentration in 120 minutes, 12.6% of the initial Cu^{2+} concentration, and 18.5%

of the initial Cd^{2+} concentration in 90 minutes, while 10.4% of the initial Zn^{2+} concentration in 60 minutes. With regard to affinity for the adsorbent, Pb^{2+} has the highest, followed by Cu^{2+} and Cd^{2+}, while Zn^{2+} has the lowest. All the metals displayed a greater breakthrough time in AC-SDS than AC. This is because the AC-SDS has extra binding sites for the adsorption of heavy metals as a result of the incorporation of SDS on AC.

Figure 11 shows the outlet heavy metal concentration against the adsorption time for a 20 cm bed height. For the AC, in 120 minutes, 13.2% of the initial Pb^{2+} concentration, and 14.4% of the initial Cu^{2+} concentration appears in the outlet stream. In 60 minutes, 11% of the initial Zn^{2+} concentration, and 22.1% of the

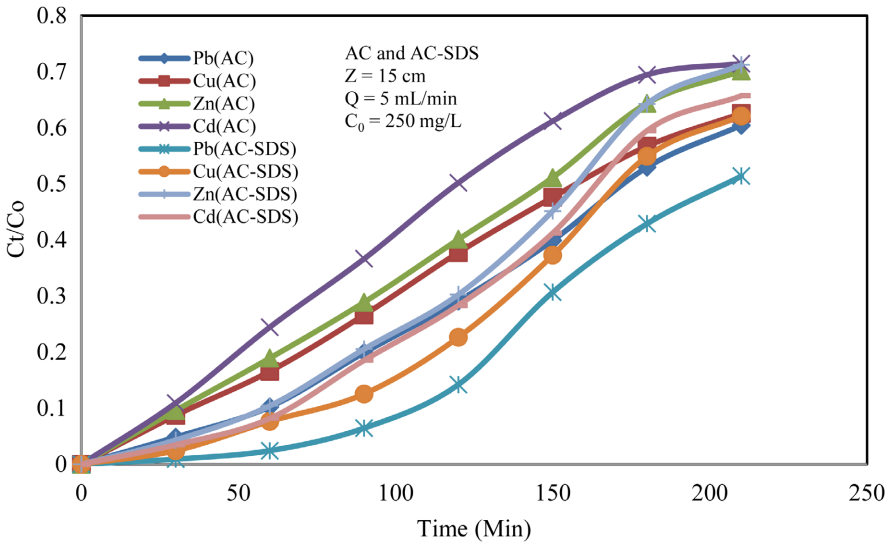

Figure 10. Breakthrough curve for simultaneous adsorption of heavy metals (Pb, Cu, Zn and Cd) onto AC and AC-SDS: Effect of bed height (Q = 5 mL/min; C_0 = 250 mg/L, Z = 15 cm).

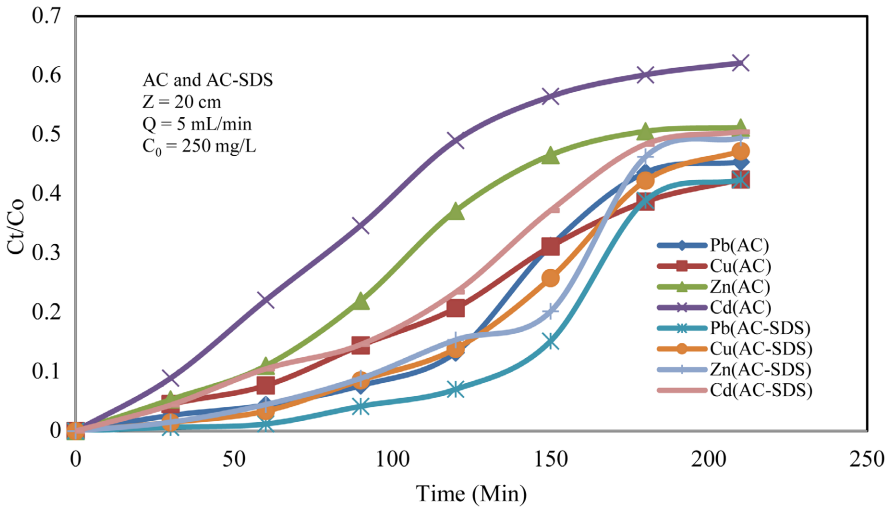

Figure 11. Breakthrough curve for simultaneous adsorption of heavy metals (Pb, Cu, Zn and Cd) onto AC and AC-SDS: Effect of bed height (Q = 5 mL/min; C_0 = 250 mg/L, Z = 20 cm).

initial Cd^{2+} concentration show up in the outlet stream. That means, with regard to affinity for the adsorbent, Pb^{2+} has the highest, followed by Cu^{2+}, and Zn^{2+} while Cd^{2+} has the lowest.

Similarly, for the AC-SDS, the outlet stream contains 15.2% of the initial Pb^{2+} concentration in 150 minutes, 13.9% of the initial Cu^{2+} concentration, and 15.4% of the initial Zn^{2+} concentration in 120 minutes, while 10.5% of the initial Cd^{2+} concentration show up in 60 minutes. With regard to affinity for the adsorbent, Pb^{2+} has the highest, followed by Cu^{2+} and Zn^{2+} while Cd^{2+} has the lowest. Again all the metals shown greater breakthrough time on AC-SDS than AC because the AC-SDS has more binding sites for the adsorption of heavy metals as a result of the incorporation of SDS on AC.

Generally as shown in **Figures 9-11** increase in bed height from 10 - 20 cm caused an increase in the breakthrough time for all the metals in both the AC and SDS-AC. This is due to an increase in the surface area and the number of binding sites available for adsorption. The time for interaction of adsorbate and adsorbent also increased with increasing amount of adsorbent [35] [36]. Compared to the SDS-AC, the breakthrough time of the AC is lower. This is explained by the incorporation of SDS on the AC, which gives the heavy metals additional binding sites.

3.4.3. Effect of Initial Concentration on the Adsorption of the Heavy Metal Ions

Figure 12 shows the outlet heavy metal ions concentration against the adsorption time for a 50 mg/L initial metal concentration. For the AC, in 150 minutes, 10.4% of the initial Pb^{2+} concentration appears in the outlet stream. In 120 minutes, 10.3% of the initial Cu^{2+} concentration, and 14.3% of the initial Zn^{2+} concentration

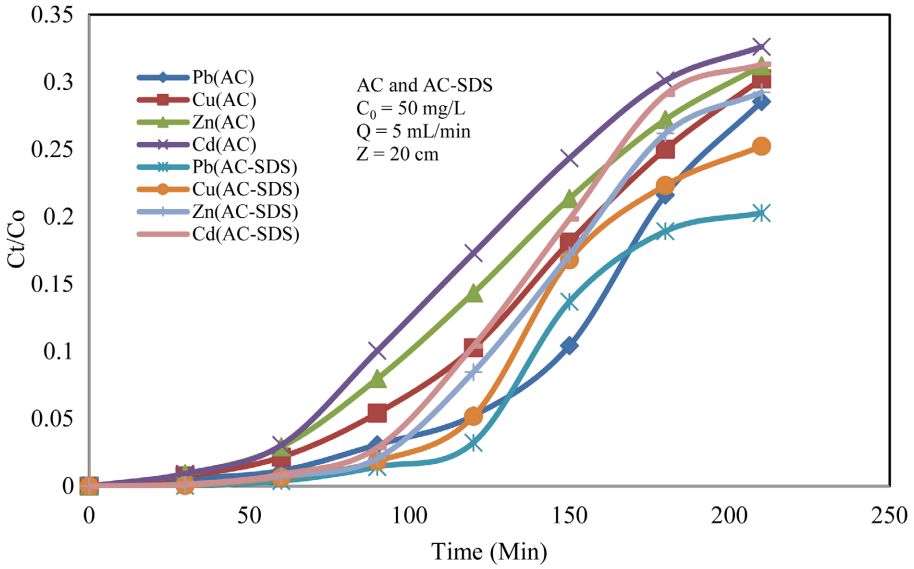

Figure 12. Breakthrough curve for simultaneous adsorption of heavy metals (Pb, Cu, Zn and Cd) onto AC and AC-SDS: Effect of initial concentration (Q = 5 mL/min; C_0 = 50 mg/L, Z = 20 cm).

shows up in the outlet stream. In 90 minutes, 10.1% of the initial Cd^{2+} concentration appears in the outlet stream. With regard to affinity for the adsorbent, Pb^{2+} has the highest, followed by Cu^{2+} and Zn^{2+}, while Cd^{2+} exhibits the lowest.

Similarly, for the AC-SDS, in 150 minutes, 13.7% of the initial Pb^{2+} concentration, 16.8% of the initial Cu^{2+} concentration, and 17.2% of the initial Zn^{2+} concentration appears in the outlet stream. In 120 minutes, 10.4% of the initial Cd^{2+} concentration shows up in the outlet stream. With regard to affinity for the adsorbent, Pb^{2+} exhibits the highest, followed by Cu^{2+} and Zn^{2+}. while Cd^{2+} has the lowest. On AC-SDS as opposed to AC, every metal displayed a greater break through time because the AC-SDS has additional binding sites for the adsorption of heavy metals as a result of the incorporation of SDS on AC.

Figure 13 shows the outlet heavy metal concentration against the adsorption time for a 150 mg/L initial metal concentration. For the AC, in 150 minutes, 18.2% of the initial Pb^{2+} concentration appears in the outlet stream. In 120 minutes, 14.7% of the initial Cu^{2+} concentration shows up in the outlet stream. In 90 minutes, 11% of the initial Zn^{2+} concentration, and 11.3% of the initial Cd^{2+} shows up in the outlet stream. That means Pb^{2+} has the highest affinity for the adsorbent, followed by Cu^{2+} and Zn^{2+}, while Cd^{2+} has the lowest.

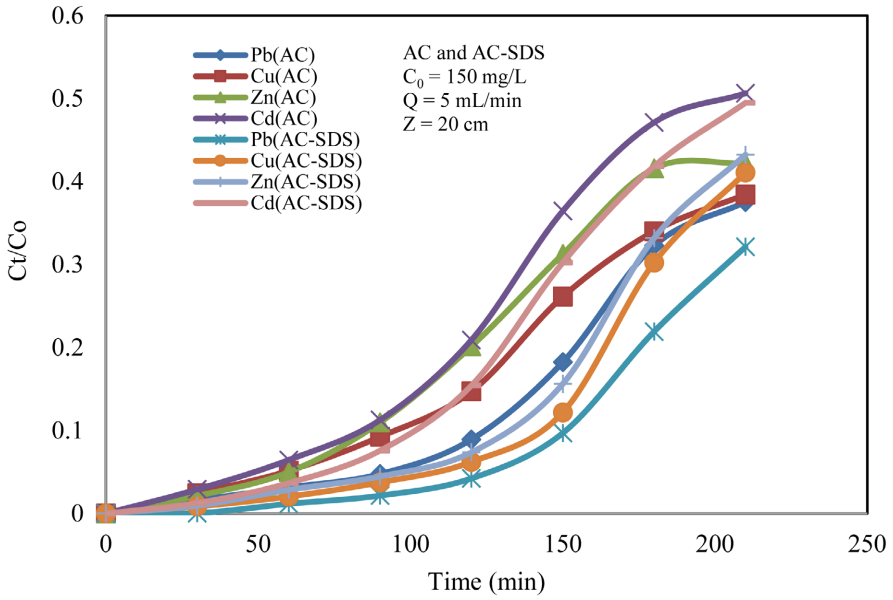

Figure 13. Breakthrough curve for simultaneous adsorption of heavy metals (Pb, Cu, Zn and Cd) onto AC and AC-SDS: Effect of initial concentration (Q = 5 mL/min; C_0 = 150 mg/L, Z = 20 cm).

Similarly, for the AC-SDS, the outlet stream contains 21.9% of the initial Pb^{2+} concentration in 180 minutes. A 12.2% of the initial Cu^{2+} concentration, and 15.6% of the initial Zn^{2+} in 150 minutes. In 120 minutes, 15.4% of the initial Cd^{2+} concentration shows up in the outlet stream. That indicates that Pb^{2+} has the highest affinity for the adsorbent, followed by Cu^{2+} and Zn^{2+} while Cd^{2+} has the lowest. Again on AC-SDS as opposed to AC, every metal displayed a greater break

through time. This is because the AC-SDS has more binding sites for the adsorption of heavy metals as a result of the incorporation of SDS on AC.

Figure 14 shows the outlet heavy metal concentration against the adsorption time for a 250 mg/L initial metal concentration. For the AC, in 120 minutes, 13.2% of the initial Pb^{2+} concentration appears in the outlet stream. In 90 minutes, 14.4% of the initial Cu^{2+} concentration shows up in the outlet stream while in 60 minutes, 11% of the initial Zn^{2+} concentration and 22.1% of the initial Cd^{2+} appear in the outlet stream. With regard to affinity for the adsorbent, Pb^{2+} has the highest, followed by Cu^{2+} and Zn^{2+} while Cd^{2+} has the lowest.

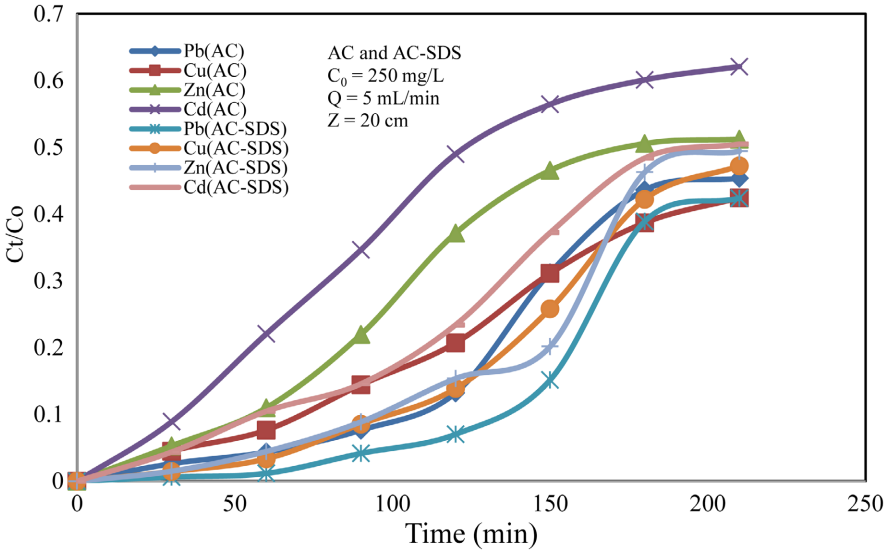

Figure 14. Breakthrough curve for simultaneous adsorption of heavy metals (Pb, Cu, Zn and Cd) onto AC and AC-SDS: Effect of initial concentration (Q = 5 mL/min; C_0 = 250 mg/L, Z = 20 cm).

Similarly, for the SDS-AC, the outlet stream contains in 150 minutes, 15.2% of the initial Pb^{2+} concentration, in 120 minutes, 13.9% of the initial Cu^{2+} and 15.4% of the initial Zn^{2+} concentration. In 60 minutes 10.5% of the initial Cd^{2+} appear in the outlet stream. That shows that Pb^{2+} exhibits the highest, followed by Cu^{2+} and Zn^{2+} while Cd^{2+} has the lowest. Every metal ion displayed a greater break through time on AC-SDS than AC because the more binding sites AC-SDS than AC for the adsorption of heavy metals as a result of the incorporation of SDS on AC.

The breakthrough time was shortened when the concentration was increased from 50 to 250 mg/L for all the metals ions on both AC and AC-SDS. Less treated synthetic waste water is produced in the event of a lower break through volume, which is indicated by a lower break through time. Initially, adsorption was rapid due to the availability of a large number of empty binding sites. Thereafter, increase in initial adsorbate concentration results in a greater driving force to overcome mass-transfer resistance in the liquid phase, and the sites are exhausted quickly, so the volume of effluent treated also decreases [37] [38].

Overall, the affinity of the heavy metals to both AC and AC-SDS followed the

order of $Pb^{2+} > Cu^{2+} > Zn^{2+} > Cd^{2+}$. This affinity order conforms to what was obtained during simultaneous adsorption of these four heavy metals to zeolite synthesized from high calcium fly ash [39]. The crystal structure, ionic hydration radius, and hydration-free energy of the materials largely contribute to their selectivity [40]. Panayotova [41] found that for metal ions, the adsorption affinity increased with decreasing hydration radius and hydration-free energy. The selectivity should be Pb^{2+} (0.401 nm) > Cu^{2+} (0.419 nm) > Cd^{2+} (0.426 nm) > Zn^{2+} (0.430 nm) in relation to the size of the hydrated radius. Nevertheless, this order does not provide a satisfactory explanation for why Zn^{2+} has a higher selectivity than Cd^{2+}. The higher selectivity could be attributed to the hydration-free energy of Zn^{2+} (−2044 KJ/mol) being lower than that of Cd^{2+} (+979 KJ/mol) [42] [43].

4. Conclusion

Sodium dodecyl sulfate (SDS) surfactant incorporation onto the surface of activated carbon enhances its capacity for simultaneous adsorption of Pb^{2+}, Cu^{2+}, Zn^{2+}, and Cd^{2+} from an aqueous medium in an expanded bed column. The affinity of the heavy metals to both AC and AC-SDS followed the order of Pb^{2+}, Cu^{2+}, Zn^{2+}, and Cd^{2+}. The dynamic adsorption of the column depends on the flow rate, bed height, initial metal concentration, and SDS surface modification. With a 5 mL/min flow rate, a 20 cm bed height, and a 50 mg/L initial metal concentration, a maximum break-through time of 150 minutes for the unmodified activated carbon (AC) and 180 minutes for the SDS-modified activated carbon (AC-SDS) was reached.

Acknowledgements

The Tertiary Education Trust Fund (TETFund) of Nigeria was acknowledged by the authors for its support in funding sample analysis, logistics, and the acquisition of equipment and reagents.

Conflicts of Interest

The authors declare no conflicts of interest regarding the publication of this paper.

References

[1] Goel, J., Kadirvelu, K., Rajagopal, C. and Kumar Garg, V. (2005) Removal of Lead(II) by Adsorption Using Treated Granular Activated Carbon: Batch and Column Studies. *Journal of Hazardous Materials*, **125**, 211-220. https://doi.org/10.1016/j.jhazmat.2005.05.032

[2] Patel, H. (2020) Batch and Continuous Fixed Bed Adsorption of Heavy Metals Removal Using Activated Charcoal from Neem (*Azadirachta indica*) Leaf Powder. *Scientific Reports*, **10**, Article No. 16895. https://doi.org/10.1038/s41598-020-72583-6

[3] Renu Agarwal, M., Singh, K., Gupta, R. and Dohare, R.K. (2020) Continuous Fixed-Bed Adsorption of Heavy Metals Using Biodegradable Adsorbent: Modeling and Experimental Study. *Journal of Environmental Engineering*, **146**, No. 2. https://doi.org/10.1061/(asce)ee.1943-7870.0001636

[4] Fatimah, I., Yahya, A., Akista, R. and Sasti, T. (2017) Preparation of Sodium Dodecyl Sulphate-Functionalized Activated Carbon from GnetumGnemon Shell for Dye Adsorption. *International Conference on Chemistry, Chemical Process and Engineering* (*IC3PE*), **1823**, Article ID: 020125.

[5] Patel, H. (2019) Fixed-Bed Column Adsorption Study: A Comprehensive Review. *Applied Water Science*, **9**, Article No. 45. https://doi.org/10.1007/s13201-019-0927-7

[6] Allalou, O., Miroud, D., Belmedani, M. and Sadaoui, Z. (2018) Performance of Surfactant-modified Activated Carbon Prepared from Dates Wastes for Nitrate Removal from Aqueous Solutions. *Environmental Progress & Sustainable Energy*, **38**, S403-S411. https://doi.org/10.1002/ep.13090

[7] Chen, W., Zhang, Z., Li, Q. and Wang, H. (2012) Adsorption of Bromate and Competition from Oxyanions on Cationic Surfactant-Modified Granular Activated Carbon (GAC). *Chemical Engineering Journal*, **203**, 319-325. https://doi.org/10.1016/j.cej.2012.07.047

[8] Salam, K.A. (2019) Assessment of Surfactant Modified Activated Carbon for Improving Water Quality. *Journal of Encapsulation and Adsorption Sciences*, **9**, 13-34. https://doi.org/10.4236/jeas.2019.91002

[9] Monser, L. and Adhoum, N. (2002) Modified Activated Carbon for the Removal of Copper, Zinc, Chromium and Cyanide from Wastewater. *Separation and Purification Technology*, **26**, 137-146. https://doi.org/10.1016/s1383-5866(01)00155-1

[10] Yang, L., Wu, S. and Chen, J.P. (2007) Modification of Activated Carbon by Polyaniline for Enhanced Adsorption of Aqueous Arsenate. *Industrial & Engineering Chemistry Research*, **46**, 2133-2140. https://doi.org/10.1021/ie0611352

[11] Afkhami, A., Madrakian, T., Amini, A. and Karimi, Z. (2008) Effect of the Impregnation of Carbon Cloth with Ethylenediaminetetraacetic Acid on Its Adsorption Capacity for the Adsorption of Several Metal Ions. *Journal of Hazardous Materials*, **150**, 408-412. https://doi.org/10.1016/j.jhazmat.2007.04.123

[12] Amuda, O.S., Giwa, A.A. and Bello, I.A. (2007) Removal of Heavy Metal from Industrial Wastewater Using Modified Activated Coconut Shell Carbon. *Biochemical Engineering Journal*, **36**, 174-181. https://doi.org/10.1016/j.bej.2007.02.013

[13] Mu, G.N. and Tang, L.B. (2002) Adsorption of Cd(ii) Ion and Its Complex Compounds from Solution on the Surface of Charcoal Treated with an Oxidation-Negative Ionizing Method. *Journal of Colloid and Interface Science*, **247**, 504-506. https://doi.org/10.1006/jcis.2001.8078

[14] Youssef, A.M., El-Nabarawy, T. and Samra, S.E. (2004) Sorption Properties of Chemically-Activated Carbons. *Colloids and Surfaces A*: *Physicochemical and Engineering Aspects*, **235**, 153-163. https://doi.org/10.1016/j.colsurfa.2003.12.017

[15] Nadeem, M., Mahmood, A., Shahid, S.A., Shah, S.S., Khalid, A.M. and McKay, G. (2006) Sorption of Lead from Aqueous Solution by Chemically Modified Carbon Adsorbents. *Journal of Hazardous Materials*, **138**, 604-613. https://doi.org/10.1016/j.jhazmat.2006.05.098

[16] Hong, H., Kim, H., Baek, K. and Yang, J. (2008) Removal of Arsenate, Chromate and Ferricyanide by Cationic Surfactant Modified Powdered Activated Carbon. *Desalination*, **223**, 221-228. https://doi.org/10.1016/j.desal.2007.01.210

[17] Choi, H., Cho, J., Baek, K., Yang, J. and Lee, J. (2009) Influence of Cationic Surfactant on Adsorption of Cr(VI) onto Activated Carbon. *Journal of Hazardous Materials*, **161**, 1565-1568. https://doi.org/10.1016/j.jhazmat.2008.04.067

[18] Ahn, C.K., Park, D., Woo, S.H. and Park, J.M. (2009) Removal of Cationic Heavy

Metal from Aqueous Solution by Activated Carbon Impregnated with Anionic Surfactants. *Journal of Hazardous Materials*, **164**, 1130-1136. https://doi.org/10.1016/j.jhazmat.2008.09.036

[19] Nadeem, M., Shabbir, M., Abdullah, M.A., Shah, S.S. and McKay, G. (2009) Sorption of Cadmium from Aqueous Solution by Surfactant-Modified Carbon Adsorbents. *Chemical Engineering Journal*, **148**, 365-370. https://doi.org/10.1016/j.cej.2008.09.010

[20] Olatunji, M.A., Salam, K.A. and Evuti, A.M. (2024) Continuous Removal of Pb (II) and Cu (II) Ions from Synthetic Aqueous Solutions in a Fixed-Bed Packed Column with Surfactant-Modified Activated Carbon. *Separation Science and Technology*, **59**, 561-579. https://doi.org/10.1080/01496395.2024.2329790

[21] Musah, M. (2011) Kinetic Study of the Adsorption of Pb^{2+} and Cr^{3+} Ions on Palm Kernel Shell Activated Carbon. *Researcher*, **3**, 1-6.

[22] Adesanmi, A.S., Evuti, A.M., Aladeitan, Y.M. and Abba, A.H. (2020) Utilization of Waste in Solving Environmental Problem: Application of Banana and Orange Peels for the Removal of Lead(II) Ions from Aqueous Solution of Lead Nitrate. *Nigeria Journal of Engineering Science and Technology Research*, **6**, 18-33.

[23] Bondar, Y., Kuzenko, S., Han, D. and Cho, H. (2014) Development of Novel Nanocomposite Adsorbent Based on Potassium Nickel Hexacyanoferrate-Loaded Polypropylene Fabric. *Nanoscale Research Letters*, **9**, Article No. 180. https://doi.org/10.1186/1556-276x-9-180

[24] Bhattacharyya, P., Chakrabarti, K., Chakraborty, A., Tripathy, S. and Powell, M.A. (2008) Fractionation and Bioavailability of Pb in Municipal Solid Waste Compost and Pb Uptake by Rice Straw and Grain under Submerged Condition in Amended Soil. *Geosciences Journal*, **12**, 41-45. https://doi.org/10.1007/s12303-008-0006-9

[25] Kakavandi, B., Raofi, A., Peyghambarzadeh, S.M., Ramavandi, B., Niri, M.H. and Ahmadi, M. (2018) Efficient Adsorption of Cobalt on Chemical Modified Activated Carbon: Characterization, Optimization and Modeling Studies. *Desalination and Water Treatment*, **111**, 310-321. https://doi.org/10.5004/dwt.2018.22238

[26] Arneli,, Safitri, Z.F., Pangestika, A.W., Fauziah, F., Wahyuningrum, V.N. and Astuti, Y. (2017) The Influence of Activating Agents on the Performance of Rice Husk-Based Carbon for Sodium Lauryl Sulfate and Chrome (CR) Metal Adsorptions. *IOP Conference Series*: *Materials Science and Engineering*, **172**, Article ID: 012007. https://doi.org/10.1088/1757-899x/172/1/012007

[27] Kandah, M.I., Shawabkeh, R. and Al-Zboon, M.A. (2006) Synthesis and Characterization of Activated Carbon from Asphalt. *Applied Surface Science*, **253**, 821-826. https://doi.org/10.1016/j.apsusc.2006.01.015

[28] Castro-Castro, J.D., Macías-Quiroga, I.F., Giraldo-Gómez, G.I. and Sanabria-González, N.R. (2020) Adsorption of Cr(VI) in Aqueous Solution Using a Surfactant-Modified Bentonite. *The Scientific World Journal*, **2020**, Article ID: 3628163. https://doi.org/10.1155/2020/3628163

[29] Kareem, K.A. (2016) Removal and Recovery of Methylene Blue Dye from Aqueous Solution using Avena Fatua Seed Husk. *Ibn Al-Haitham Journal for Pure & Applied Science*, **29**, 179-194.

[30] Javadian, H., Ruiz, M. and Sastre, A.M. (2017) Sorption of Pb (II) from Aqueous Solution by Nio/Activated Carbon Nanocomposite. *Proceedings of the* 2*nd World Congress on Civil, Structural, and Environmental Engineering*, Barcelona, 2-4 April 2017, No. AWSPT 112. https://doi.org/10.11159/awspt17.112

[31] Zhou, Y., Wang, Z., Hursthouse, A. and Ren, B. (2018) Gemini Surfactant-Modified Activated Carbon for Remediation of Hexavalent Chromium from Water. *Water*, **10**, Article 91. https://doi.org/10.3390/w10010091

[32] López-Cervantes, J., Sánchez-Machado, D.I., Sánchez-Duarte, R.G. and Correa-Murrieta, M.A. (2017) Study of a Fixed-Bed Column in the Adsorption of an Azo Dye from an Aqueous Medium Using a Chitosan–glutaraldehyde Biosorbent. *Adsorption Science & Technology*, **36**, 215-232. https://doi.org/10.1177/0263617416688021

[33] Ahmad, A.A. and Hameed, B.H. (2010) Fixed-bed Adsorption of Reactive Azo Dye onto Granular Activated Carbon Prepared from Waste. *Journal of Hazardous Materials*, **175**, 298-303. https://doi.org/10.1016/j.jhazmat.2009.10.003

[34] Sheng, L., Zhang, Y., Tang, F. and Liu, S. (2018) Mesoporous/microporous Silica Materials: Preparation from Natural Sands and Highly Efficient Fixed-Bed Adsorption of Methylene Blue in Wastewater. *Microporous and Mesoporous Materials*, **257**, 9-18. https://doi.org/10.1016/j.micromeso.2017.08.023

[35] Fat'hi, M.R., Asfaram, A., Hadipour, A. and Roosta, M. (2014) Kinetics and Thermodynamic Studies for Removal of Acid Blue 129 from Aqueous Solution by Almond Shell. *Journal of Environmental Health Science and Engineering*, **12**, Article No. 62. https://doi.org/10.1186/2052-336x-12-62

[36] Teutscherova, N., Houška, J., Navas, M., Masaguer, A., Benito, M. and Vazquez, E. (2018) Leaching of Ammonium and Nitrate from Acrisol and Calcisol Amended with Holm Oak Biochar: A Column Study. *Geoderma*, **323**, 136-145. https://doi.org/10.1016/j.geoderma.2018.03.004

[37] Moyo, M., Pakade, V.E. and Modise, S.J. (2017) Biosorption of Lead(II) by Chemically Modified Mangifera Indica Seed Shells: Adsorbent Preparation, Characterization and Performance Assessment. *Process Safety and Environmental Protection*, **111**, 40-51. https://doi.org/10.1016/j.psep.2017.06.007

[38] Saravanan, A., Kumar, P.S. and Yaswanthraj, M. (2017) Modeling and Analysis of a Packed-Bed Column for the Effective Removal of Zinc from Aqueous Solution Using Dual Surface-Modified Biomass. *Particulate Science and Technology*, **36**, 934-944. https://doi.org/10.1080/02726351.2017.1329243

[39] Ji, X.D., Ma, Y.Y., Peng, S.H., Gong, Y.Y. and Zhang, F. (2017) Simultaneous Removal of Aqueous Zn^{2+}, Cu^{2+}, Cd^{2+}, and Pb^{2+} by Zeolites Synthesized from Low-Calcium and High-Calcium Fly Ash. *Water Science and Technology*, **76**, 2106-2119. https://doi.org/10.2166/wst.2017.361

[40] Hui, K., Chao, C. and Kot, S. (2005) Removal of Mixed Heavy Metal Ions in Wastewater by Zeolite 4A and Residual Products from Recycled Coal Fly Ash. *Journal of Hazardous Materials*, **127**, 89-101. https://doi.org/10.1016/j.jhazmat.2005.06.027

[41] Panayotova, M.I. (2001) Kinetics and Thermodynamics of Copper Ions Removal from Wastewater by Use of Zeolite. *Waste Management*, **21**, 671-676. https://doi.org/10.1016/s0956-053x(00)00115-x

[42] Volkov, A.G., Paula, S. and Deamer, D.W. (1997) Two Mechanisms of Permeation of Small Neutral Molecules and Hydrated Ions across Phospholipid Bilayers. *Bioelectrochemistry and Bioenergetics*, **42**, 153-160. https://doi.org/10.1016/s0302-4598(96)05097-0

[43] Tansel, B. (2012) Significance of Thermodynamic and Physical Characteristics on Permeation of Ions during Membrane Separation: Hydrated Radius, Hydration Free Energy and Viscous Effects. *Separation and Purification Technology*, **86**, 119-126. https://doi.org/10.1016/j.seppur.2011.10.033